Special Issue Article

Numerical simulation of a regional train in cross-wind

Sándor Eichinger[1], Mikael Sima[2] and Frank Thiele[3]

Abstract

In this work numerical investigations of regional trains were carried out studying the prediction accuracy of the aerodynamic load in cross-wind assessment of rail vehicles. The main focus is on 30° yaw angle. Two domain setups, one representing the wind tunnel setup and another more generic one, were investigated and validated against available measurements comparing load coefficients. Important aspects of a guideline assessing aerodynamic load coefficients with numerical simulation techniques are proposed. Based on practical considerations and on the presented results the use of a generic domain is suggested for virtual certification. Further improvement of the flow field prediction can be achieved using unsteady hybrid numerical techniques, such as detached eddy simulation. Load coefficient results of various unsteady approaches and comparisons of simulated and measured flow fields are shown. Hints about the usage of the employed hybrid method are given, and future investigations are proposed.

Introduction

The determination of the aerodynamic characteristics of trains used in the assessment of cross wind currently largely relies on static tests from wind tunnels. Whereas numerical simulations are now an integral part in the design of trains it has been more restrictive in vehicle authorisation. Numerical simulations using Reynolds-averaged Navier–Stokes (RANS) approaches are allowed in EN14067-6[1] for trains up to 200 km/h, but not at all in the HS RST TSI (2008). The use of numerical simulations for deriving aerodynamic coefficients has been explored in several studies over the last decade and more, see e.g. the review by Diedrichs.[2] It has been shown that trains can be predicted with reasonable accuracy. The comparisons though are limited in train shapes, most studies are of streamlined trains, and in yaw angle range. In some cases there are still uncertainties about the actual conditions of the test.

The presented results are based on the EU-funded project in railway aerodynamics AeroTRAIN, however some of the unsteady results were extended after the project end. The AeroTRAIN studies included wind tunnel tests and a broad range of train shapes and yaw angles. The results give a broader picture of the accuracy that can be achieved from current standard simulation approaches and the dependence on shape and yaw angle.[3,4] It was found that blunt trains are more challenging than streamlined and that the roof arrangement can add to the challenge.

The results are for 30° yaw angle, which is both challenging and in the range of most critical yaw angles for cross-wind performance.

Regional train

Regional trains have a blunt shape. They usually travel at moderate speed and are equipped with various additional features as roof boxes that are not "streamlined" and increase the aerodynamic load as well as influence the flow field. The vehicle model shown in Figure 1 was selected to represent regional trains, and is here also denoted regional train. It has a blunt frontal part, a box on the roof and simplified bogies.

Computational method

In the presented work steady RANS simulations are used, which are able to predict quasi-steady viscous

[1]qpunkt Deutschland GmbH, branch office Stuttgart, Germany
[2]Centre of competence Aero and Thermodynamics, Bombardier Transportation, Västerås, Sweden
[3]Department of Fluid Mechanics and Engineering Acoustics (ISTA), Technische Universität Berlin, Berlin, Germany

Corresponding author:
Sándor Eichinger, qpunkt Deutschland GmbH, branch office Stuttgart, Talstrasse 1, 70825 Korntal-Münchingen, Germany.
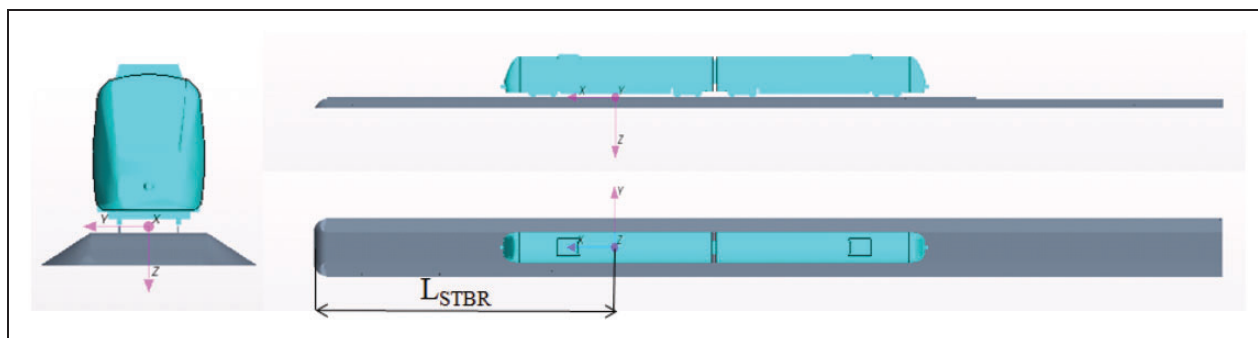Email: sandor.eichinger@qpunkt.at

Figure 1. Regional train model on single track ballast and rails.

turbulent three-dimensional flows in general. The commercial flow solver package STAR-CCM v5.06.009 developed by CD-Adapco company is employed which covers many of the current fluid mechanical application fields and also provides pre- and post-processing tools for users.

In the current cases the Mach number is moderate $Ma \leqslant 0.3$, thus the flow can be considered as incompressible. For incompressible and mildly compressible flows, using STAR-CCM v5.06.009, it is advised in the user guide[5] due to computational resource considerations to use a model in which the pressure and velocity flow equations are solved in an uncoupled manner. The linkage between momentum and continuity equations is achieved with an iterative (predictor–corrector) approach. The formulation can be described as using collocated variables and Rhie-and-Chow-type pressure–velocity coupling combined with a SIMPLE-type algorithm.[6]

Thermal effects in this instance are negligible, therefore isothermal, gravity-free simulations are sufficient.

In the case of RANS simulations the governing equations are statistically averaged to obtain a solution for the mean flow, where the effect of the turbulence is modelled. The non-linear term of the convective acceleration, known as Reynolds stresses, have to be approximated. The most commonly used models are based on the eddy viscosity concept.

Two equation models that have become industry standard models are $k - \epsilon$ and $k - \omega$. They are based on the Boussinesq eddy viscosity assumption which says that the Reynolds stress tensor is proportional to main strain rate tensor and the link is the turbulent or eddy viscosity. This eddy viscosity is computed from two transported variables which are most often: k (turbulent kinetic energy) and a second one that determines the scale of turbulence, can be either the eddy dissipation ϵ or the specific dissipation ω.

The $k - \epsilon$ model has been shown to be useful for free-shear layer flows with relatively small pressure gradients. Similarly, for wall-bounded and internal flows, the model gives good results only in cases where mean pressure gradients are small; accuracy is believed to be reduced for flows containing large adverse pressure gradients.[7]

One reported advantage of the $k - \omega$ model over the $k - \epsilon$ model is its improved performance for boundary layers under adverse pressure gradients. Perhaps the most significant advantage, however, is that it may be applied throughout the boundary layer, including the viscous-dominated region, without further modification. Furthermore, the standard $k - \omega$ model can be used in this mode without requiring the computation of wall distance. The biggest disadvantage of the $k - \omega$ model, in its original form, is that boundary-layer computations are very sensitive to the values of ω in the free stream. This translates into extreme sensitivity to inlet boundary conditions for internal flows, a problem that does not exist for the $k - \epsilon$ models. A combination of $k - \epsilon$ and $k - \omega$ two-equation model[8] is when the ϵ transport equation from the $k - \epsilon$ turbulence model is transformed into a ω transport equation and replaced into the $k - \omega$ turbulence model. In this case an additional non-conservative cross-diffusion term arises, which is included far from walls but not included near the wall and is determined by a blending function. The use of a $k - \omega$ formulation in the inner parts of the boundary layer makes the model directly usable all the way down to the wall through the viscous sublayer. The shear stress transport (SST) formulation also switches to a $k - \epsilon$ behaviour in the free-stream and thereby avoids the common $k - \omega$ problem of over-sensitivity to the inlet free-stream turbulence properties. Authors who use the SST $k - \omega$ model often merit it for its good behaviour in adverse pressure gradients and separating flow. In the presented work Menter's SST- $k - \omega$ two equation model and second-order upwind convective discretisation is employed. A suitable wall function for all dimensionless distances values is used.

Transient methods

Steady-state simulations are advantageous due to their short turnaround times and due to their applicability in predicting trends. When transient effects are important unsteady techniques may significantly improve the quality of the obtained results. Unsteady RANS (URANS) equations are applicable

to transient situations such as imposed unsteadiness or largely separated flows.

Detached eddy simulation (DES) is a hybrid modelling approach, which is a combination of RANS and large eddy simulation (LES). The method can be briefly described as the following: the near-wall regions are modelled with the help of the base RANS turbulent closure, in the separated flow regime if the mesh is fine enough a sub-grid scale model is used similar to LES approaches.

In the presented work two of the numerous implemented DES formulations into STAR-CCM v5.06.009 were employed: the Delayed DES (DDES) using the Spalart–Almaras (SA) model[9] and the DES formulation of the SST $k - \omega$ model.[10] The details of the implementations are not available however the formulations are given in the STAR-CCM Manual.[5] During the project work a comparison was made of the given formulation regarding the hybrid convective scheme with that from Travin et al.,[11] which pointed out the following: in STAR-CCM a C_{desT} coefficient takes a default value of 1.0, which is very conservative while in the original publication the equivalent value is 0.1. This C_{desT} coefficient therefore should to be adjusted in order to ensure that the central-based convection scheme is activated in the flow regions where it is possible. In the presented work due to time restrictions this value was adjusted only for the DDES-SA approach.

In order to avoid relaminarisation of the turbulent structures due to too large physical time stepping a proper definition of the used time resolution during the transient run is essential.

In the case of DES simulations based on the given grid size near the lee-side of the Regional Train and the used physical time step the resulting CFL number was about 1.65. For the URANS case the time resolution is less critical therefore a coarser time step based on the generic bluff body's Strouhal number of 0.1 together with the inflow velocity and the grid cell size was determined.

As for the steady-state investigations the thermal effects are considered to be negligible, therefore isothermal, gravity free simulations are performed. In the case of DDES-SA model for the spatial discretisation the hybrid central convective (HCD) scheme was used which is a combination of second-order upwind and pure central differencing schemes depending on a blending coefficient computed locally in the flow based on theoretical considerations.[11] It provides good accuracy for the computation of the convective fluxes of the flow equations. In case of DES-SST the bounded HCD scheme was employed, which is more robust than the HCD scheme however might be less accurate. The temporal discretisation was second-order accurate.

Computational domain

The computational domains used are shown in Figure 2, where one is representing the experimental setup (WT), see Figure 2(a) and the other a generalised domain (GD), see Figure 2(b). The cross section of a single track ballast and rails (STBR) follows requirements in EN14067-6,[1] whereas the upstream length is more than the minimum required.

For the presented simulations a computational domain model with 1:15 scale was used.

The coordinate system used to determine the aerodynamic forces and moments is defined according to EN14067-6.[1] The origin is located at the centreline of the vehicle, at the top of the rail level and midway between the bogies for the measured vehicle, as shown in Figure 1. The geometrical scaling of the aerodynamic loads and moments are based on the characteristic length $l = 3$ m and area $A = 10 \, \text{m}^2$ in full scale. Further loads and pressure coefficients are scaled with the inlet velocity in GD, and the velocity above the vehicle near the ceiling in WT. The lee rail roll coefficient computed as $C_{Mx,lee} = C_{Mx} - C_{Fz} \, b_0/l$ is the rolling moment coefficient about the lee rail, where the distance $2b_0 = 1.5 \, \text{m}$ defines the nominal lateral distance between the contact points of a wheel set for standard gauge track of 1435 mm. Both domains used are in 1:15 scale.

The computational domain should be defined so the boundaries do not interfere with the flow around the vehicle. To ensure that, the following recommendations are given EN14067-6.[1]

- The domain should be extended in the stream wise direction relative to the vehicle at least 8 characteristic heights upstream and 16 characteristic heights downstream, where characteristic length is defined by the distance from the maximum height of the train to the top of rail.
- The resulting blockage ratio for a yaw angle of $30°$ shall be less than 15%.

These recommendations can be easily fulfilled in case of numerical simulations. However, when wind tunnel data are available and validation simulations must be performed the domain should represent the actual wind tunnel setup.

To model the actual geometrical setup of the available measurement (see the Experimental setup section), a domain was constructed as is shown in Figure 2(a). The given non-dimensional distances based on $l = 3$ m are $L_{SPL,U} = 25$, $L_{SPL} = 15.95$, $L_{SPL,D} = 33.33$, $W = 15$, $B = 8.33$ and $H_{SPL} = 1.165$. The splitter plate leading edge has the radius of $R_{SPL} = 0.125$. The vehicle coordinate system has a distance from the splitter plate leading edge of $L_{TR,U} = 8.45$. The region under the splitter plate and its pressure drop is approximated with a porous material. At the beginning of the project a flow qualification were done in order to validate the method based on measured flow profiles. It has been found that the best match can be achieved if the flow under the splitter plate is considered in the numerical
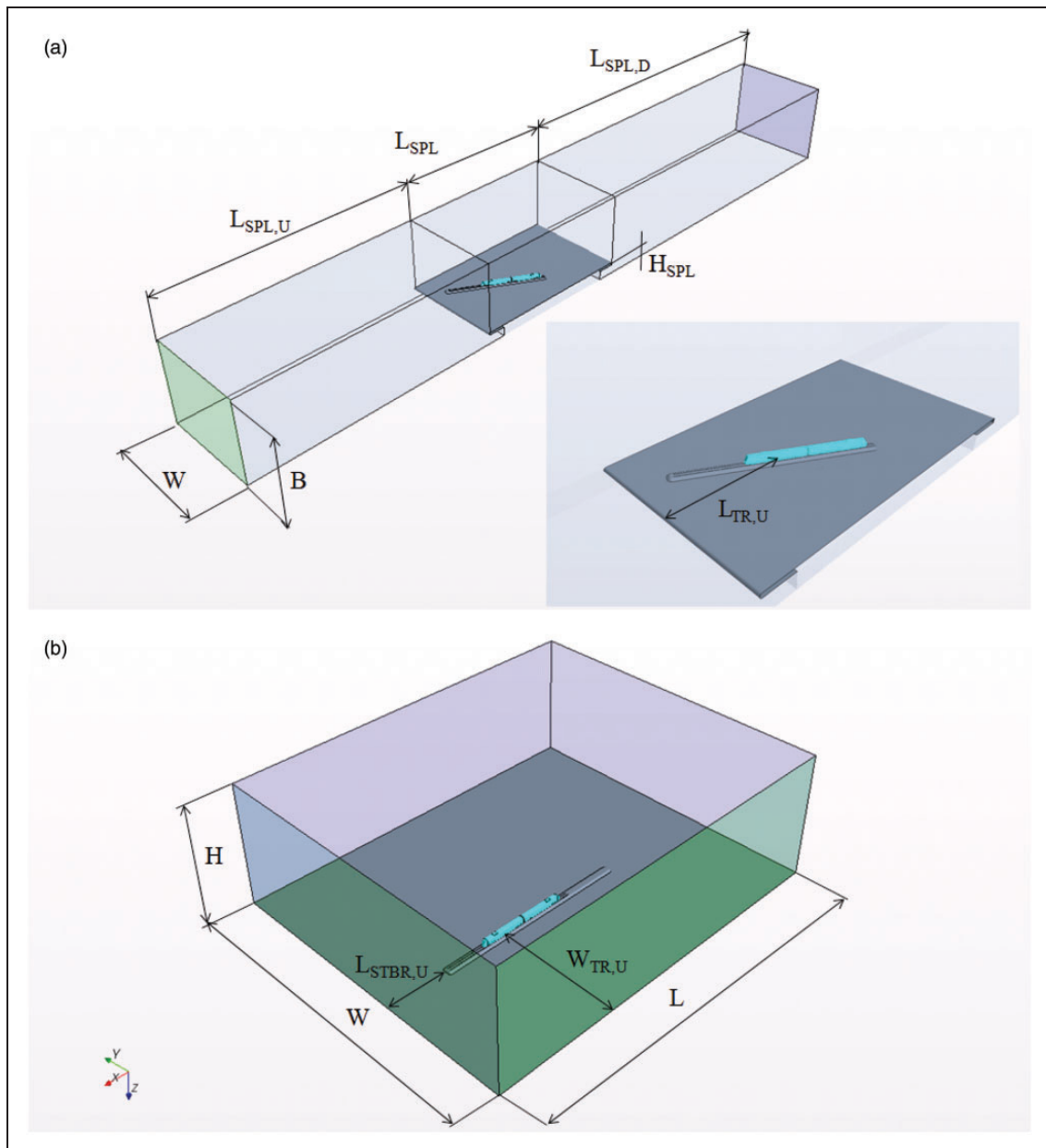
Figure 2. Used computational domains. (a) Numerical domain constructed to approximate the experimental setup (WT). (b) Generalised domain (GD).

model. When the vehicles were mounted on the splitter plate, due to the lack of pressure data in this region, the porosity value is determined to match the measured velocity over the middle of vehicle near the ceiling , see Eichinger.[14]

The WT setup is specific to one experiment. When this is not the aim it is more appropriate to use a generic domain setup, which can simple emulate more idealistic environment and more realistic ones, as well as catering for all yaw angles (Figure 2(b)). The domain consists of a rectangular volume, the investigated vehicle and the STBR. Between the STBR and the train wheels there is a gap, and in contrast to the WT domain, supporting struts and balance connections are neglected. The domain has the non-dimensional dimensions $L = 70$, $W = 58.3$,

$H = 23.3$. Over the portion of no-slip ground a boundary layer will develop. It is useful when the distance from the vehicle coordinate system to the forward inlet, $L_{TR,U}$, is the same as the distance from the middle between the rails to the upstream side boundary, $W_{TR,U} = 18.9$. The total length of the STBR is $L_{STBR} = 7.7$, and $L_{STBR,U} = 11.2$.

In GD the STBR does not extend to the forward boundary. The downstream end of the STBR should be far enough from the downstream vehicle, to prevent upstream influences.

Computational grid and boundary conditions

The computational grid of the WT setup consists of polyhedral elements. The current mesh has 7–10
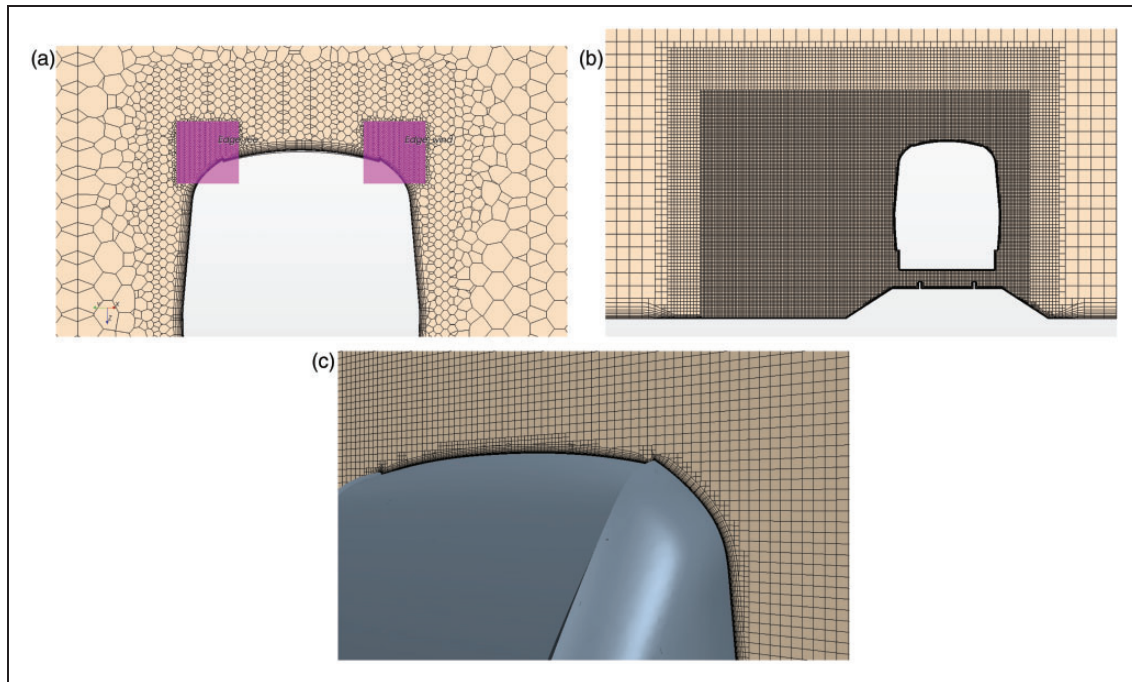
Figure 3. Mesh cuts. (a) Grid in a plane perpendicular to the train in the WT setup. (b) Grid of the GD setup in a plane perpendicular to the train. (c) Closer view of mesh.

prismatic layers adjacent to the vehicle walls, with the growth rate of 1.25. Around the vehicle and near the lee side refinement zones are defined where the mesh sizes are respectively about $\delta = 0.03$ and $\delta = 0.06$ (in non-dimensional length: the ratio of the actual cell size and the characteristic length). Further refinements near the bogies, inter-car gaps, nose, under body region and rails with $\delta = 0.015$ are applied. For a certain train geometries, especially those belonging to the less-streamlined conventional class, might exist some specific geometrical details, for instance sharp edges, boxes installed on the roof etc. It is known that local refinements may improve the final prediction. Since the regional train has such details on the roof an additional zone with even finer resolution is defined around the longitudinal edges of the roof along the whole train including the nose region as well, see Figure 3(a).

The computational grid of the GD consists of trimmed hexahedral elements, aligned with the global x-coordinate direction, with 15 prismatic cell layers around the vehicle (growth rate 1.3). Around the vehicle surface and near the lee side a refinement zone is defined where the mesh size is $\delta = 0.015$ (in non-dimensional length). Two cuts of the computational grid are shown in Figure 3(b) and (c). The grid is made also for DES wherefore it is finer than would normally be required for RANS. The grid resolution requirements are somewhat more demanding in case of DES in terms of cell size especially in the separated flow regime. According to the guidelines of Spalart[12] the energy containing large eddies require a resolution box of 32^3 cells. Since in the lee-side of the regional train a strong vortex pair is expected the

available approximately 60 cells along the regional train height is used for this investigation. A comprehensive study of the mesh resolution and further refinement was not possible within the current project, it would be the scope of future investigations.

The GD domain has a block profile velocity of 42.6 m/s on the inlet, giving a Reynolds number (based on inlet velocity and characteristic length in model scale of about $Re = 565,000$ to 600,000. On the outlet of the domain zero pressure is specified. For the WT domain an inlet velocity profile was specified equal to the experimental axial velocity. The wind tunnel has a small lateral component that is compensated by using an effective yaw angle. In the WT setup the inlet velocity has only an axial component and the train is positioned at the actual yaw angle. In case of WT the side, in order to keep the mesh size moderate, the bottom and top surfaces of the domain have a symmetry condition, while the splitter plate is a no-slip smooth wall. For the GD the vertical boundaries are inlets and outlets, the top surface symmetry and the ground no-slip smooth wall. The STBR and vehicle are in each case no-slip smooth walls.

Experimental setup

Within AeroTRAIN Task 3.2 the aerodynamic forces and moments of the regional train among many others were measured in the Jules Verne Climatic Wind Tunnel (WT) of CSTB in Nantes. The measurement campaign took place in the dynamic circuit, more precisely in the closed "high-speed" test section. The maximum velocity was at half power about 45 m/s. The sketch of the wind tunnel and pictures
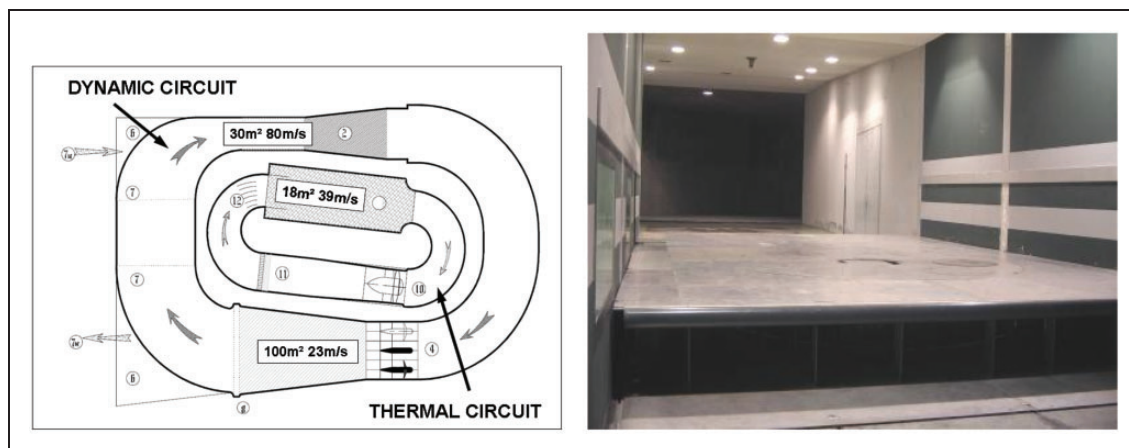
Figure 4. Experimental setup (source: CSTB Report [13]). (a) Jules Verne Climatic Wind Tunnel of CSTB. (b) High-speed test section with a splitter plate.

of the test section with the splitter plate are given in Figure 4. The investigations were carried out at 1:15 model scale. The full results are presented in the CSTB Report.[13]

The test section has a height of 5 m and a width of 6 m. The splitter plate level is at 0.7 m from the ground. The splitter plate upstream length is 9.57 m. The six-component balance which was employed during the experiment is located under the splitter plate, together with numerous supporting struts. At the leading edge of the splitter plate a half-cylinder is mounted with the diameter of 15 cm.

The coordinate system which is used to determine the aerodynamic forces and moments are defined according to EN14067-6[1] as for the numerical simulations.

The regional train wind-tunnel model consists of two cars. They are identical as they are mirrored about the mid-point of the inter car gap. Lateral symmetry is requested by the EN14067-6 standard.[1] The upstream vehicle is connected to the balance with four cylindrical struts. The second or downstream vehicle does not have a mechanical contact with the first car. The gap between the cars is 5 mm at the model scale. The second or downstream vehicle is supported by four simplified cylindrical struts, which were adjustable according to the vehicle position.

During the measurement campaign not only the data from the 6-component balance (force and moment coefficients) were collected. Additionally, in several predefined positions pressure tap data were also obtained, and in two positions perpendicular to the train longitudinal axis the flow field was measured using a particle image velocimetry (PIV) technique.

Results

The comparison of the results obtained with different numerical simulation techniques and experiments is given in the following subsections.

Table 1. Force and moment coefficient results of RANS-SST validation simulations in the WT.

Yaw angle	C_x [-]	C_y [-]	C_z [-]	C_{Mx} [-]	$C_{Mx,lee}$ [-]
20°	−0.29	3.15	−1.70	1.90	2.33
30°	−0.36	6.57	−2.18	3.91	4.46
40°	−0.71	9.54	−2.93	5.76	6.49
50°	0.26	11.3	−3.27	6.84	7.65

Validation of numerical approach

As a first step an extensive numerical parameter study has been performed in order to validate and derive a setup which can be used as a base configuration for further investigation during the project work. The complete study can be found in Eichinger,[4] and it is not presented here completely. The investigated numerical parameters were: the prism cell growth rate, the number of prism layers, the thickness of prism layers, the meshing approach, and the turbulence model. The study and validation was performed using the WT-domain setup, and it resulted in the computational grid, see the section on "Computational grid and boundary conditions".

During the numerical parameter study the yaw angle was fixed to 30°. Subsequently the result of the study the mentioned derived setup was applied to further yaw angles. The resulting force and load coefficients are given in Table 1 and the corresponding differences relative to the available measurements are given in Table 2.

One can see that at larger yaw angles (30–50°) the numerical simulation and the experiment differs noticeably. The lift force is underestimated while the side force and roll moment are higher than measured. The overall effect on $C_{Mx,lee}$ being 6–14% higher than measured. It can be either due to the fact that the used

Table 2. Comparison of coefficients relative to experiments for RANS-SST simulations in WT.

Yaw angle	ΔC_y [%]	ΔC_z [%]	ΔC_{Mx} [%]	$\Delta C_{Mx,lee}$ [%]
20°	4.11	−6.51	9.63	6.28
30°	12.7	−22.5	16.3	9.60
40°	8.93	−20.3	14.7	9.30
50°	11.7	−16.8	18.7	13.5

Table 3. Force and moment coefficient results of RANS-SST simulations in the WT and GD at 30° yaw.

Domain	C_x [-]	C_y [-]	C_z [-]	C_{Mx} [-]	$C_{Mx,lee}$ [-]
GD	−0.22	6.85	−2.35	4.07	4.66
WT	−0.36	6.57	−2.18	3.91	4.46

Table 4. Comparison of force and moment coefficients relative to experiments for RANS-SST simulations.

Domain	ΔC_y [%]	ΔC_z [%]	ΔC_{Mx} [%]	$\Delta C_{Mx,lee}$ [%]
GD	17.5	−16.5	21.1	14.6
WT	12.7	−22.5	16.3	9.6

RANS approach struggles in the case of largely separated flows, or due to the mismatch of boundary conditions between the experiment and the idealised numerical setup.

Influence of computational domain

In Table 3 the relative force and moment coefficients obtained with the mentioned GD and WT setups at 30° are given. The relative differences between the computed load coefficients with the CSTB wind tunnel measurements are shown in Table 4.

One can see that the lee-rail moment coefficient of the WT case is closer to the measurement value by 5%. The rolling moment coefficient about the coordinate system origin is smaller by 4.8% in case of WT domain. The side force coefficient is about 4.8% smaller than for the GD. The predicted lift coefficient difference in the case of the WT domain is larger about 6%. The resulting differences are due to the velocity profiles reaching the train. As was mentioned in the section on "Computational domain" the WT domain is constructed in a similar manner to the experimental setup. At the leading edge of the splitter plate a half-cylinder is mounted which causes a specific flow pattern reaching the train especially near the under-body. Although the WT geometry is not the perfect representation of the experimental conditions it has an influence on the load coefficients. In addition, as described in the previous section, the computational meshing approaches and the refinement zones were different which may also have an influence on these discrepancies.

Derivation of guidelines

When validating the accuracy of the numerical approach, an accurate representation of the actual WT domain reduces differences due to geometrical modelling. However, for assessing vehicles for acceptance, it is better to use the potential of simulations to employ exactly the same domain for all vehicles. In that case the more idealised GD is suitable. It has further advantages: it is not only applicable for all yaw angles using the same grid, but more complex inflow profiles including wind gusts or atmospheric boundary layers can be easily implemented as well.

A check of Eichinger[4] show that the resolution of the ground, even with the increasing cell size towards the domain boundaries, is sufficient to have little influence on the boundary layer and therefore the evolving flow profile development. It is rather the length of the no-slip ground that matters. Although the length of the upstream no-slip ground could in principle be used to improve a comparison with measurements, one of the benefits with computational fluid dynamics (CFD) and the generalised domain is the possibility to achieve the same conditions for any train.

For this reason, the upstream length of the no-slip ground should be limited to a certain value. The length of 70 m, as is included in the recommendations by Eichinger,[14] gives a small enough boundary layer at the train. With this length, the distance is sufficient to place the inlet boundaries at the same distance, obviating the need for a slip ground. A slip ground section, moving the no-slip ground section closer to the train, could be used to reduce the boundary layer even further. Although not deemed necessary, if it is done the axial and lateral upstream length of the no-slip part should be kept equal. In the generalised domain there is no special restriction to the STBR, therefore it is recommended to make the portion ahead of the train longer than the minimum requirement for wind tunnels, e.g. 20 m in full scale.

As a good practice based on the currently presented and the extensive simulations performed by Eichinger,[4] recommendations regarding the following with more details are given in Eichinger.[14]

- Computational domain: the use of the simplified GD, STBR, coordinate system, load coefficients.
- Computational mesh: details of refinement zones, meshing approach, boundary layer mesh.
- Computational method: the turbulence model, boundary conditions, Inflow treatment, Reynolds numbers that should be used.

● The simulation convergence should be controlled properly.

If these suggestions are kept in mind during the numerical evaluation of aerodynamic characteristics of a train similar to the regional train used here one can ensure a reliable level of accuracy and quality regarding the numerical investigation.

Advanced simulation techniques

Within AeroTRAIN Task 3.3 (T3.3) of Work Package-3 cross-winds, the aim was to check the accuracy of state-of-the-art RANS CFD approaches for vehicle acceptance. In this section since some vehicle configurations were found to be challenging for the presented RANS approaches, the aim is to investigate and explore the improvements that can be gained with simulation approaches such as URANS, DES and DDES at a given representative yaw angle of 30°. The 30° yaw angle is chosen as it was one of the most challenging to predict with steady approaches as well as being very relevant for the vehicle assessment. Initial investigations of these more advanced methods were also performed within AeroTRAIN, and were continued after the project end. The main results are presented in the following subsection.

In Table 5 the most important load coefficient are given for the regional train with various transient approaches and also for the above described steady RANS method using the identical mesh setup of GD. The relative differences compared with the available measurement are given in Table 6.

The unsteady RANS methodology provides mean load coefficients with even larger discrepancies than when using a steady approach. This is somehow the opposite of what is expected, even though it is well known that the turbulence models used have difficulties for such largely separated flows.

Using the DES method the predicted mean load coefficients are closer to the experimental values. The RANS part of the DES approach plays an important role, since the values of the DES-SST

method are somewhat closer to the experiments. These values were however obtained with the previously mentioned default C_{desT} value. The resulting flow field is therefore mostly computed with RANS models. Also, the available time period for obtaining the mean values were smaller than for the DDES-SA method due to the time restrictions, resulting in a larger uncertainty regarding the given load coefficient values.

The most reliable results are the one obtained using the DDES-SA approach. The time history of the computed force and load coefficients are given in Figures 5 and 6. One can see that for this instance the number of samples available for obtaining the mean values were sufficient including approximately four or five convective units (based on train length).

Comparisons between the available PIV measurements and the flow field of the DDES-SA case are shown in Figures 7 and 8. The measurement planes are located on the lee side of the train 5 and 11 m from the vehicle nose in full scale. The iso-lines or contours of the velocity magnitude are plotted with continuous

Table 6. Comparison of force and moment coefficients with the experiments for the simulated cases.

Case	ΔC_y [%]	ΔC_z [%]	ΔC_{Mx} [%]	$\Delta C_{Mx,lee}$ [%]
RANS SST	17.5	−16.5	21.1	14.6
URANS SST	20.9	−19.7	25.4	17.6
DES SST	12.4	−11.7	16.0	11.2
DDES SA	15.6	−8.0	19.5	14.8

Table 5. Force and moment coefficient results of simulated cases.

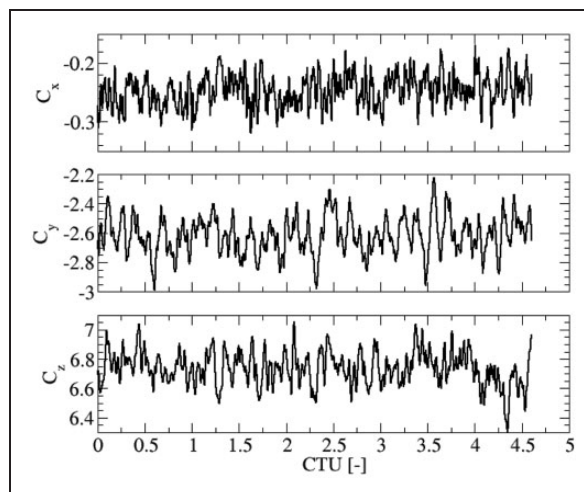| Case	C_x [-]	C_y [-]	C_z [-]	C_{Mx} [-]	$C_{Mx,lee}$ [-]
RANS SST	−0.22	6.9	−2.35	4.07	−4.66
URANS SST	−0.24	7.0	−2.26	4.22	−4.78
DES SST	−0.26	6.6	−2.48	3.90	−4.52
DDES SA	−0.25	6.7	−2.59	4.02	−4.67

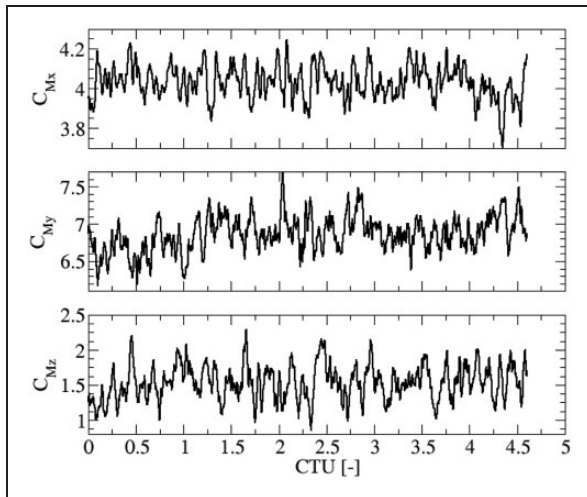**Figure 5.** Force coefficients using the DDES-SA approach.

Figure 6. Moment coefficients using the DDES-SA approach.

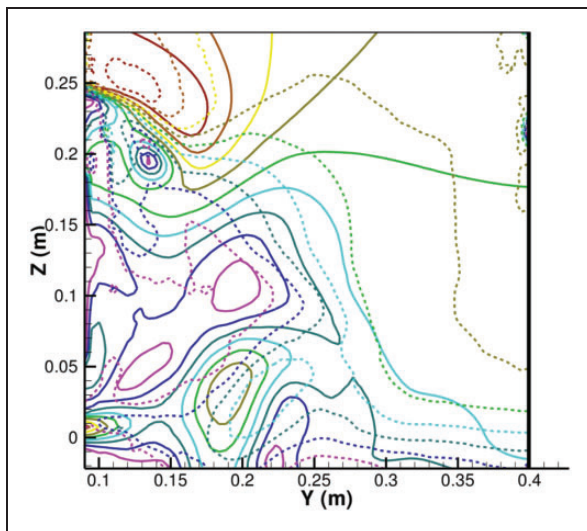**Figure 8.** Velocity contour line comparison at $x = -0.187$ m slice cut: full line, DDES-SA; dotted line: experiment.

Figure 7. Velocity contour line comparison at $x = -0.787$ m slice cut: full line, DDES-SA; dotted line, experiment.

Figure 9. Instantaneous $\lambda 2$ iso-surface near the regional train for DDES-SA.

and dotted lines for the simulation and experiment respectively. Close to the vehicle front at $x = -0.787$ m one can observe the upper lee vortex positioned near to the body. Further downstream at $x = -0.187$ m the vortex is larger and additionally an even larger lower vortex appears. The simulated flow field have a good agreement with the measured flow.

Pressure-based vortex visualisation technique was used to help further understanding the flow around the given vehicle configuration. The instantaneous $\lambda 2 = -1500$ iso-surfaces of the DDES-SA approach are shown in Figure 9. With the current numerical settings: spatial and time resolution, and the adjusted C_{desT} value the resolved structures can be seen fine. The instability vortices near the blunt nose can be observed. Also the quasi-steady separation near the roof box and along the windward roof edge of the regional train are lightly recognisable.
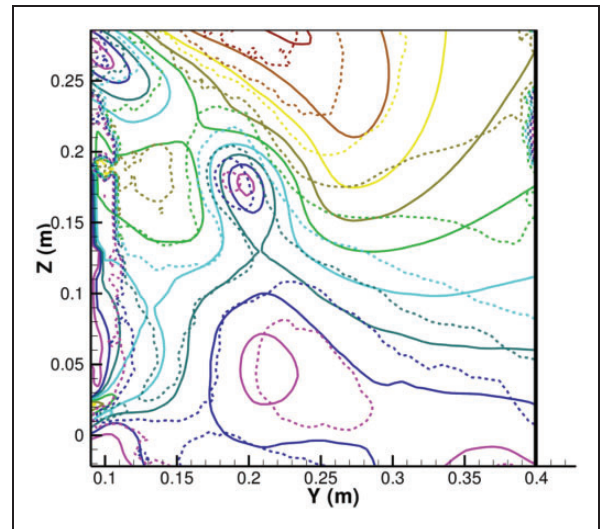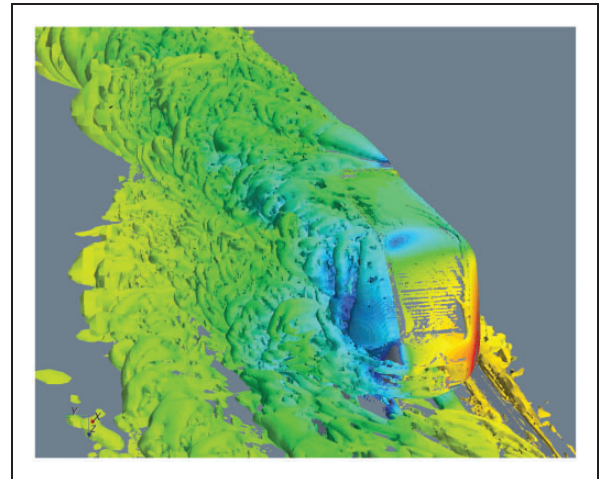
Conclusions

It has been shown that for the given specific blunt train and yaw angle numerical simulation using the RANS methodology can be used for the prediction of load coefficients with a reasonable level of accuracy. For validation purposes an accurate representation of the actual measurement set-up is advantageous, however for assessment of the aerodynamic characteristics a generalised domain is recommended. The details of these suggestions can be found in the guidelines by Eichinger.[14]

Hybrid numerical simulation techniques, specifically DES, might be an alternative to the presented work. Despite the large computational effort required by these techniques they can deliver qualitatively finer results than the steady approaches. There can be specific problems for example, blunt trains with roof

equipment in strong side wind when the predictions can be improved.

These methods should be further investigated, since important aspects such as the influence of further mesh refinements were not investigated due to the limited time at the end of the project work. There are indications that further improvements in the prediction can be attained. A comprehensive study of the numerous available hybrid techniques could further clarify the potential and give more guidance about suitable settings for the application to cross wind.

References

1. EN14067-6. *Railway Applications – Aerodynamics – Part 6: Test procedures and requirements for aerodynamics on open track*. European Standard, 2010.
2. Diedrichs B. *Computational Methods for Crosswind Stability of Railway Trains. A Literature Survey*. Stockholm: Royal Institute of Technology (KTH), 2005, p.27.
3. Sima M, Eichinger S, Blanco A and Ali I. *WP3 – T3.3 CFD simulations Output document* AeroTRAIN project publication D6.3(I), A3.3., 2012.
4. Eichinger S. *CFD validation investigations on VT 612 and IC4*. Internal AeroTRAIN report AEROTRAIN-WP3-R3.3.1, Aerotrain Project, 2012.
5. STAR-CCM+ User Guide, Version 5.06.009, CD Adapco, 2011.
6. Ferziger JH and Peric M. *Computational Methods for Fluid Dynamics*, 3rd revised edn. Berlin: Springer-Verlag, 2002.
7. Wilcox DC. *Turbulence modelling for CFD*. DCW Industries, Incorporated, 1994.
8. Menter FR. Two-equation eddy-viscosity turbulence modeling for engineering applications. *AIAA Journal* 1994; 32(8): 1598–1605.
9. Spalart PR, Deck S, Shur ML, Squires KD, Strelets M and Travin A. A new version of detached eddy simulation, resistant to ambiguous grid densities. *Theor Comput Fluid Dynamics* 2006; 20: 181–185.
10. Menter FR and Kuntz M. Adaptation of eddy viscosity models of unsteady separated flows behind vehicles. *The Aerodynamics of Heavy Vehicles: Trucks, Buses and Trains*. Asilomar, CA: Springer, 2002.
11. Travin A, Shur S, Strelets ML and Spalart PR. Physical and numerical upgrades in the in the detached eddy simulation of complex turbulent flows. In *Proceedings of the 412th Euromech Colloquium on LES and Complex Transitional and Turbulent Flows*, Munich, Germany, 2000.
12. Spalart PR. *Young person's guide to detached-eddy simulation grids*. NASA contractor report, NASA/CR-2001-211032, 2001.
13. Aguinaga S. *Wind tunnel tests for aerodynamic loads on trains due to crosswinds*. AeroTRAIN project, 2011.
14. Eichinger S. *D3.3.1(1) CFD investigations: validated procedures for assessing aerodynamic coefficients*. Aerotrain Project, 2012.